

18. Googarchin, H. S. and Ghajar, R., Stress intensity factors calculation for surface crack in cylinders under longitudinal gradient pressure using general point load weight function. *Fatigue Fract. Eng. M.*, 2014, **37**(2), 184–194.
19. Heng, S., Yang, C. H., Guo, Y. T., Wang, C. Y. and Wang, L., Influence of bedding planes on hydraulic fracture propagation in shale formations. *Chin. J. Rock Mech. Eng.*, 2015, **34**(2), 228–237.
20. Sih, G. C., Pairs, P. C. and Irwin, G. R., On cracks in rectilinearly anisotropic bodies. *Int. J. Fract. Mech.*, 1965, **1**(3), 189–203.
21. Dai, F. and Xia, K. W., Laboratory measurements of the rate dependence of the fracture toughness anisotropy of Barre granite. *Int. J. Rock Mech. Min. Sci.*, 2013, **60**, 57–65.
22. Ministry of Water Resources of the People's Republic of China, *Specifications for Rock Tests in Water Conservancy and Hydroelectric Engineering*, China Standards Press, Beijing, 2007.
23. Chong, K. P., Kuruppu, M. D. and Kuszmaul, J. S., Fracture toughness determination of layered materials. *Eng. Fract. Mech.*, 1987, **28**(1), 43–54.

ACKNOWLEDGEMENTS. This research was funded by the China Postdoctoral Science Foundation Funded Project (No. 2016M592402), Hubei Provincial Natural Science Foundation of China (Nos 2016AHB015, 2016CFA013), and Wuhan Science and Technology Bureau (No. 2016070204020156).

Received 9 January 2017; revised accepted 21 April 2017

doi: 10.18520/cs/v113/i06/1153-1159

## Deformational characteristics of Donglingxin slope induced by reservoir fluctuation and rainfall

J. Yu<sup>1</sup>, R. B. Wang<sup>1,\*</sup>, J. C. Zhang<sup>2</sup>, L. Yan<sup>1</sup>, Q. X. Meng<sup>1</sup>, C. Zhang<sup>1</sup> and X. Z. Li<sup>3</sup>

<sup>1</sup>Research Institute of Geotechnical Engineering, Hohai University, Nanjing 210098, China

<sup>2</sup>College of Water Conservancy and Hydropower Engineering, Hohai University, Nanjing 210098, China

<sup>3</sup>Zhongnan Engineering Corporation Limited, PowerChina, Changsha 410014, China

**Landslides induced by reservoir inundation and rainfall are very common in southwest China, adversely affecting the construction of hydropower plants in this area. In this study, a case of Donglingxin slope located at the Sanbanxi reservoir is reported, which developed into a large landslide. To understand deformation and conduct stabilization measurement, an in-depth study has been done based on monitoring the trigger events like reservoir fluctuation, rainfall and groundwater levels. It was revealed that the rainfall mainly affected deformation of the upper slope; reservoir fluctuation**

**reduced the stability of the toes of the slope. The activity of groundwater between the bedrock and the soil-rock mixture, geomaterials greatly controlled the global stability. An analysis of the comprehensive effects of these trigger events, indicated that the slope was unstable and would have slid into the reservoir. The evolution of slope deformation was simulated by particle flow code, the result showed that the landslide started from the head of the gully. This case study provides important geo-technical references for engineering the prevention of reservoir bank slopes.**

**Keywords:** Donglingxin slope, deformational characteristics, reservoir bank slope, reservoir fluctuation, rainfall.

LANDSLIDE is one of the most serious geological hazards in the reservoir regions of hydropower station. Both reservoir fluctuations and rainfall infiltration become major factors that affect a landslide. Especially after impoundment, several ancient landslides are reactivated. Some huge reservoir landslide events have been previously reported<sup>1</sup>. The Zhaxi landslide induced by a reservoir killed over 70 workers in 1961 (ref. 2). The Qianjiangping landslide, also induced by a reservoir killed 24 people in 2003 (ref. 3). So the stability of reservoir slope is a major problem in China and the economic losses related to landslide are over 20 billion every year<sup>4</sup>.

According to Qi *et al.*<sup>5</sup>, the mechanical strength of sliding zone controls the deformation of landslide, and hydraulic effects deteriorate the strength of sliding zone. Taking an example of Shuping landslide, Wang *et al.*<sup>6</sup> found that the deformation of Shuping landslide corresponds to the Three Gorges reservoir fluctuations, especially, the deformation of the landslide is more active during periods of declining reservoir levels. Continuous rainfall also triggers the failure of slope, because the strength of the sliding zone is reduced by water infiltration<sup>7</sup>. Besides, Burda *et al.*<sup>8</sup> proposed that the climate change induces reactivation of landslide.

The Donglingxin slope is an ancient landslide with a volume of 20.7 million m<sup>3</sup>. It is located on the right bank of Qingshui river, Guizhou Province (Figure 1). The slope belongs to Sanbanxi hydropower project, which is about 80 km downstream of the slope. In July 2007, during the first reservoir impoundment, the ancient landslide was reactivated. The valley in the landslide region is extremely narrow, hence the support and protection measurements are difficult to be implemented. As this landslide located only 1 km from Liuchuan town with more than 30,000 inhabitants, its stability is a major safety problem. Therefore, we must analyse landslide deformation characteristics and also its potential failure.

This communication presents a comprehensive analysis of Donglingxin landslide. Based on the two-year observation data, we analysed landslide deformation and triggering mechanism related to reservoir fluctuation and rainfall. The factor of safety is calculated for stability

\*For correspondence. (e-mail: rbwang\_hhu@foxmail.com)

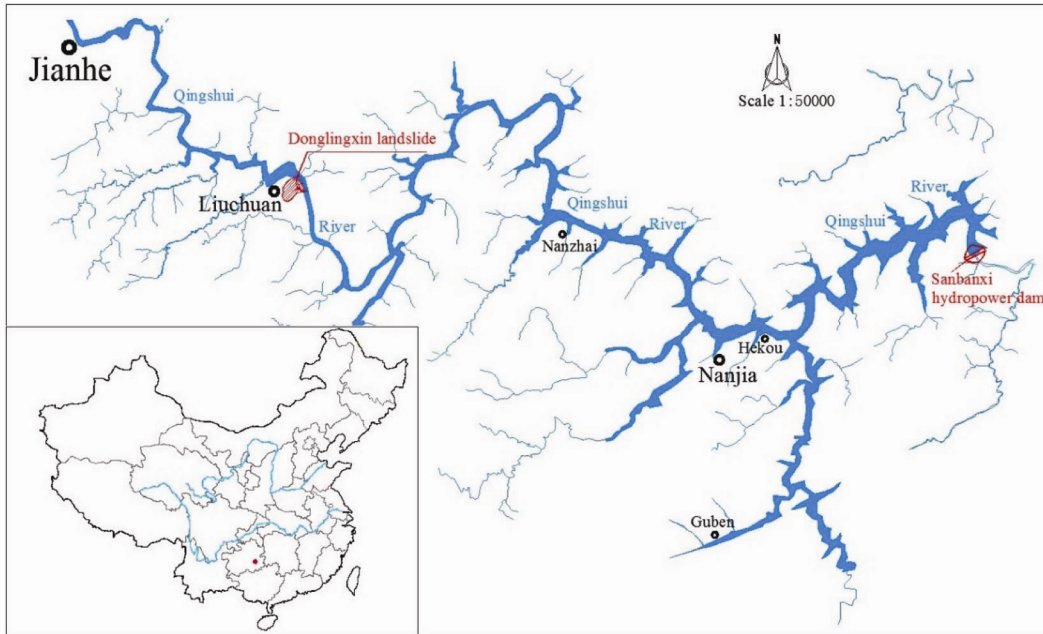


Figure 1. The location map of the Sanbanxi reservoir and Donglingxin landslide.

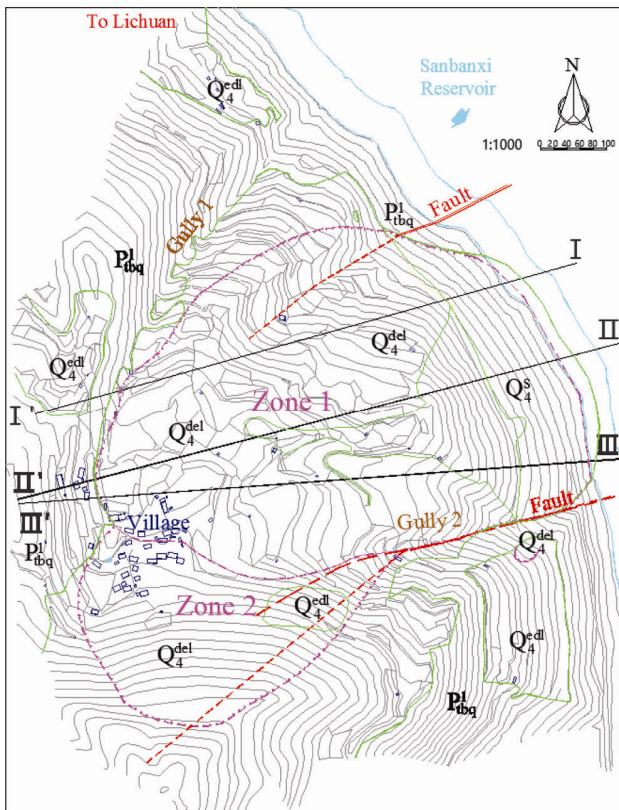


Figure 2. The plane shape map of Donglingxin slope.

analysis. Apart from this, the accumulation patterns of the slope failure were simulated by particle flow code.

As a large-scale ancient landslide (Figure 2), the morphogenic process of Donglingxin landslide is formed

by several slides along the bank slope, whose vestiges can be found in the slope toe. Graveland silty clay covered most area of landslide; clay and cataclastic rock mass mixture accumulated at the toe of the excavation slope and central ridge. As shown in Figure 3, the topography and landforms of Donglingxin landslide appear like an armchair. There are two gullies on the edge of the slope, and one of them divided the slope into two zones. The main landslide bodies located in zone 1 with a height of 280 m and an area of 310 sq. km, extend about 800 m along Qingshui river. The highest position of zone 1 is 700 m elevation. The landslide bodies located in zone 2 are only 68 sq. km in area, which is approximately one fifth of zone 1 area, and located in the upper southern part of the main landslide bodies with a height of 120–220 m and a width of 200 m. The topography of zone 2 appears like a fan. The elevation of zone 2 is around 600 to 825 m.

The stratum of Donglingxin landslide is shown in Figure 4. It mainly consists of Banxi group of Algonkian system and Quaternary strata. With different geological genesis, the strata are divided into landslide deposits ( $Q_4^{del}$ ), eluvium and diluvium deposits ( $Q_4^{edl}$ ), artificial deposits ( $Q_4^s$ ), sliding zone and bedrock. The geological material of bedrock belongs to member 1 of Qingshui Formation of Banxi group of Algonkian system ( $P_{1tbq}^1$ ). Rock soil mixture which belongs to eluvium and diluvium deposits ( $Q_4^{edl}$ ) is mainly distributed on the back edge of the slope. Most geological materials of Donglingxin landslide belong to landslide deposits ( $Q_4^{del}$ ). According to different contents and size of stone, landslide deposits ( $Q_4^{del}$ ) could be divided into three

types: (1) Rock soil mixture with a stone content of 20–40%, cover most of the surface of landslide except its toe. This mixture is composed of coarse-grained clay and broken stones, which are strongly weathered. (2) Silty clay and gravel mixture with a stone content of over 35%, is mostly covered by geological materials. The stone in this stratum is also strongly weathered. (3) Cataclastic rock mass which is mainly distributed at the toe of the slope. The rock in this stratum mainly consists of tuffaceous sandstone and tuffaceous silty slate, and its mass is relatively integrated, with moderate weathering. The sliding zone is located between bedrock and landslide deposits, and composed by silty clay and a little gravel. This stratum is about 1.3–11.3 m in thickness. Artificial deposits ( $Q_4^d$ ) are accumulated in the landslide toe, which are usually gravel from highway excavation projects.

The slope is located on a relative wet mountain area where the mean annual precipitation is about 1280.5 mm. From March to July, the maximum daily precipitation is

up to 133.3 mm during this period of significant rainfall. The water level of Sanbanxi reservoir fluctuates between 425 and 472 m. The groundwater of the slope consists of pore phreatic water and fissure water, which is influenced by precipitation and reservoir. The groundwater has two drainage paths in the slope. Water flows downwards into the bedrock through fracture network in the slope or directly into the gully of slope.

Cracks can be observed directly by *in situ* investigation. Geodetic deformity monitoring is used to measure the displacement of the slope, and borehole monitoring is used to observe the groundwater variation.

There are six concrete datum points in geodetic deformity monitoring, three of them for horizontal displacement and the other three for vertical displacement monitoring. The nine observation positions (G 01 to G 09) are shown in Figure 5. Electronic total station and digital level were used to observe the changes in displacement. For horizontal displacement datum points, the mean square error of adjacent points is  $\pm 3.0$  mm, for vertical displacement datum points, the mean square error is  $\pm 2.0$  mm; for observation points, the mean square error of horizontal displacement of adjacent points is  $\pm 6.0$  mm and vertical displacement is  $\pm 5.0$  mm. During the flood season (March–July), the monitoring frequency was once in every 15 days, and in the dry season, monitoring frequency once in every 30 days.

The observation data of displacement were recorded from October 2009. Eight boreholes were simultaneously drilled, and cables connected to a multimeter were put into these boreholes for measuring groundwater variation.

The *in situ* investigation reveals that the Donglingxin bank slope is a typical ancient landslide with noticeable geomorphology features. A bedding landslide lies on the front side of Donglingxin bank slope. After rainfall,



Figure 3. Picture of Donglingxin slope (panoramic view).

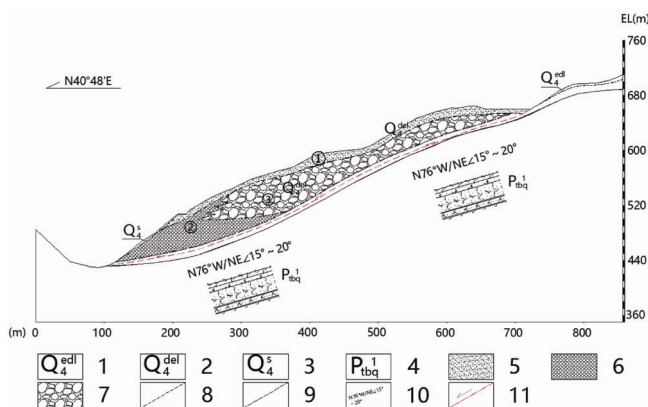


Figure 4. Geological profile of the landslide deposit (profile of I-I'). (1) Eluvium and diluvium, (2) landslide deposits, (3) human accumulation layer, (4) member 1 of Qingshui Formation of Banxi group of Algonkian system, (5) rock soil mixture with a stone content of 20–40%, (6) silty clay and gravel mixture with a stone content of over 35%, (7) cataclastic rock mass, (8) deposit boundary, (9) lithologic boundary, (10) occurrence of rock, (11) sliding zone.

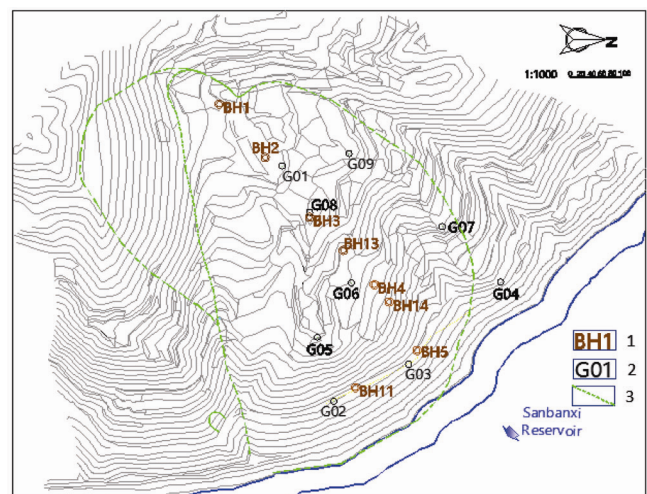
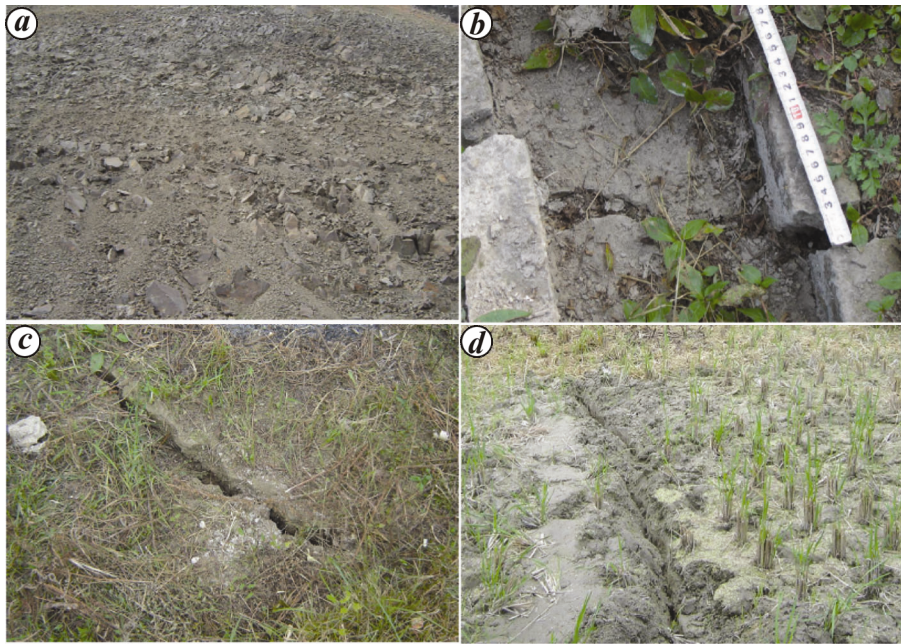
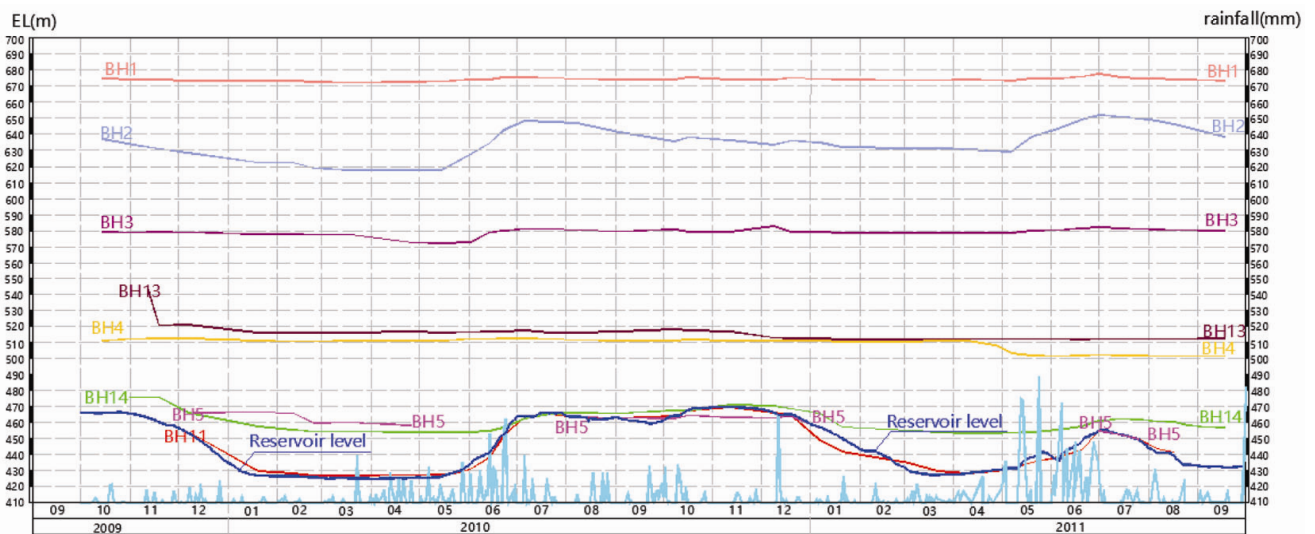


Figure 5. Location map of the boreholes and observation positions in Donglingxin slope. (1) Boreholes, (2) observation points, (3) deposit boundary.



**Figure 6.** Spot photographs of dynam-relaxed rock mass and fractures. *a*, Dynam-relaxed rock mass; *b*, Fracture in back side of zone 1; *c*, Fractures in western gully; *d*, Fractures in rice paddies.



**Figure 7.** Monitoring results of groundwater levels at boreholes BH1–BH5, BH11, BH13 and BH14 in the period of October 2009 to September 2011.

collapse often occurs in the cutting slope of Liunan highway. There is a large scale distribution of dynam-relaxed rock mass on the landslide (Figure 6 *a*), and thus deformation can be observed.

After first impoundment of Sanbanxi reservoir and a rainy season, a large deformation was observed in the Donglingxin landslide. Several new tension and shear fractures appeared on the back side of zone 1, close to the head of gully. As shown in Figure 6 *b*, the opening width of cracks ranged from 3 to 20 cm, and the visible depth of tension cracks ranged from 10 to 30 cm. Some fractures

with a width of 1–5 m and a length of 2 m, were also observed near the gully 1 (Figure 6 *c*), and extended along N10°W–N20°E. Figure 6 *d* shows a tension fracture with a visible depth of 10–30 cm observed in the rice paddies, which extended along N10°W–N5°E. Some fractures along east-west direction were also observed in zone 2 with an elevation of 740 m. The sliding surface and arc of collapse started from the fracture in the upper part of the slope, were generated in zone 1.

According to the above observations, we found that there was a creep deformation in the Donglingxin landslide.

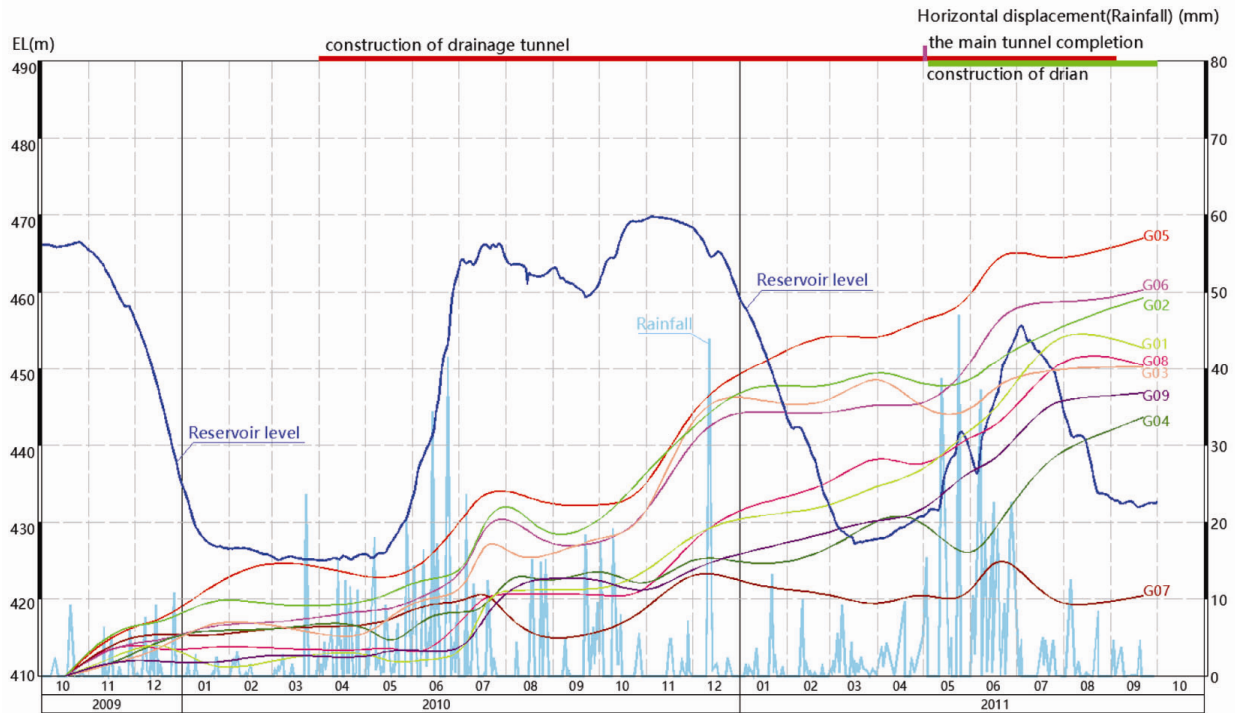


**Figure 8.** Monitoring displacements of nine observation positions in the period of October 2009 to September 2011.

After a long-term accumulation of creep deformation, disintegration and collapse may start from the toe of zone 1, and then collapse occurs in zone 2, because of the loss of supporting force from zone 1. Besides, new fractures and cracks will be generated by rainfall infiltration which will accelerate creep deformation and lead to a larger scale collapse.

From the monitoring results of groundwater and deformation (Figures 7 and 8), we found two interesting phenomena – (1) reservoir fluctuation mainly changed the groundwater in the slope toe and there was a positive correlation between reservoir and groundwater. For example, the water level of reservoir decreased from 466 to 426 m during November 2009 to February 2010 and at the same time, the groundwater in boreholes BH11 (elevation 508.62 m) dropped from 452.32 to 428.19 m. From May to July 2010, the groundwater rose by 36.17 m, while the water level of reservoir rose from 426 to 466 m. The slope toe mainly consisted of geological material 3 with high permeability due to which water infiltrated into it easily. Simultaneously, the deformation at G02 (elevation 511.7 m) and G03 (elevation 498.4 m), at the slope toe, increased rapidly from May to July 2010, because the strength of geological materials is reduced by increase in water pressure<sup>9,10</sup>. (ii) Rainfall mainly changed the groundwater in the upper part of the slope. Between May and September 2010, after a strong precipitation, groundwater in boreholes BH2 (elevation 678.35 m) located in the upper part of the slope rose to 647.88 from 617.91 m, and then declined to 634.27 m. From May to

June 2011, again after a strong precipitation, the groundwater in boreholes BH2 rose to 652.21 from 629.09 m, and then declined rapidly to 638.40 m. The upper part of slope mainly consists of geological material 1 with poor permeability. Hence, rainwater accumulation formed groundwater in the upper part, which eventually decreases in the absence of rain. Simultaneously rain infiltration increased deformation in the upper part of slope. After strong precipitation in June and September 2010, the resulting displacements were observed in the observation positions G01 (elevation 672.6 m), G08 (elevation 664.5 m) and G09 (elevation 659.9 m), all located in the upper part of the slope.

One can conclude that rainfalls and reservoir fluctuations affect different areas of the slope respectively. Both can accelerate deformation of the slope by water infiltration, and reduce its stability. The monitoring data also indicates that the Donglingxin landslide exhibits creep deformation which is accelerated by water infiltration and this lead to a large scale collapse. These agree with the results of *in situ* observation.

The deformation of Donglingxin slope is attributed to the decrease of shear strength, especially the decreasing strength of the sliding zone. The effective stress declines because the pore water pressure in sliding zone increases after water infiltration. The shear strength of geological material in Donglingxin slope is shown in Table 1. The cohesion of sliding zone is 23 kPa in natural state, after water infiltration, the cohesion declines to 20 kPa, while the friction angle decreases from 29.4° to 28°.

**Table 1.** Parameters of accumulated landslide layer

Strata	Elastic modulus (MPa)	Poisson's ratio	Shear strength					
			Cohesion (kPa)		Friction angle (°)		Density (g/cm <sup>3</sup> )	
			Natural	Saturated	Natural	Saturated	Natural	Saturated
Geological material <sup>1</sup>	26.8	0.37	20	18	26	24	2.00	2.10
Geological material <sup>2</sup>	45.3	0.36	20	15	35	30	2.15	2.22
Geological material <sup>3</sup>	50.2	0.31	20	15	33	30	2.20	2.25
Sliding zone	27.6	0.33	23	20	29.4	28	2.03	2.08

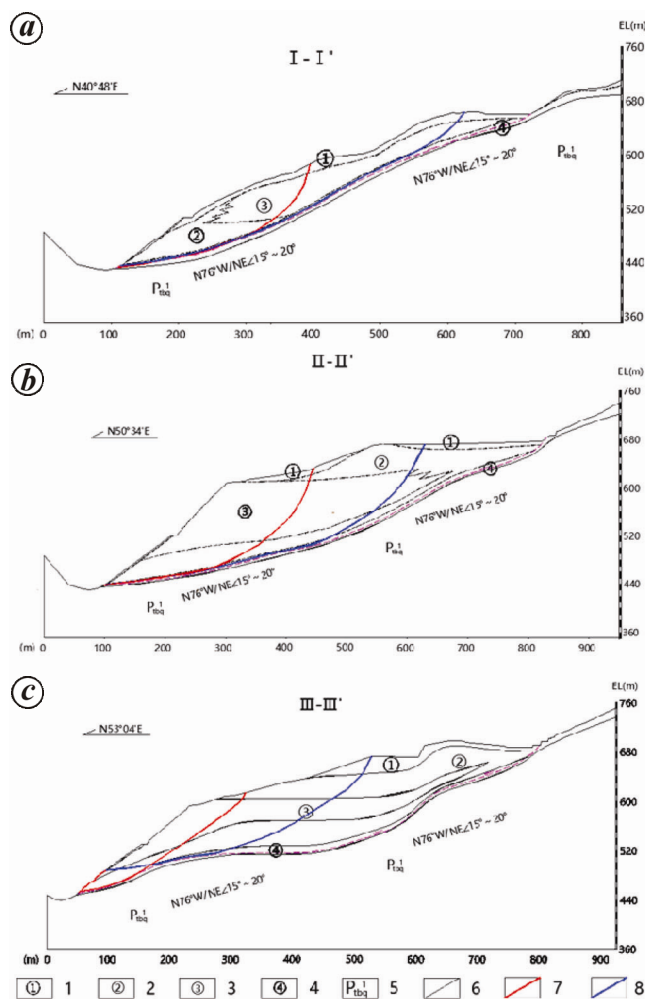


**Figure 9.** Geological profile of the landslide deposit. *a*, I–I'. *b*, II–II'. *c*, III–III'. (1) Geological material 1, (2) geological material 2, (3) geological material 3, (4) sliding zone, (5) member 1 of Qingshui formation of Banxian group of Algonkian system, (6) lithologic boundary, (7) shallow sliding surface, (8) deep sliding surface.

In order to study the stability of Donglingxin slope, we selected three typical engineering profiles (Figure 9) for calculating the factors of safety (FS). Natural, rainfall and inundation with rainfall – these three conditions are taken into account. The FS calculated by modified Janbu<sup>11</sup> method are presented in Table 2.

As the majority of sliding zone is unsaturated before rainfall or inundation, its shear strength in the natural state will be higher than that in rainfall or inundation state (Table 1). Therefore, FS in natural state will be higher than that in rainfall or inundation state (e.g. 1.133 in natural state, 1.085 in rainfall state, 1.014 in inundation with rainfall state, for profiles I–I'). As the middle part of the slide is steeper, FS of the slide after inundation and rainfall, especially of the middle part (profiles II–II'), will be reduced greatly. The FS of I–I' and III–III' are close to 1.0 (1.014 and 1.028) after inundation and rainfall, while that of II–II' is less than 1.0 (0.995). One can conclude that slope would be in critical state – there is a significant risk of landslide after inundation and rainfall. The results of stability analysis are in accordance with the observation of deformation.

As there is a significant risk of landslide after inundation and rainfall, it is important to learn the evolution of slope deformation and assess the damage of landslide. YADE<sup>12</sup> is an open-source particle flow code. By adjusting the micro particle parameters, realistic macromechanical behaviour of geological materials can be reproduced<sup>13</sup>. The damage of geological materials is simulated directly on the micromechanical scale in this approach, the complicated constitutive relationship is no more taken into account.

To simulate the deformation of Donglingxin slope, we need to simplify the geological materials. In this model, eluvium and diluvium deposits ( $Q_4^{edl}$ ) and artificial deposits ( $Q_4^s$ ) are ignored due to their small volumes, and landslide deposits ( $Q_4^{del}$ ) are considered as the geological material. For high computational efficiency, landslide deposits and the geo-materials  $P_{tbq}^1$  are regarded as particles and rigid materials respectively. The boundary of the Donglingxin landslide is explicit and a smooth transfixion sliding surface can be noticed. According to *Geological Investigation and Computation Analysis* in this paper (chapter 4), the dangerous sliding surface of the landslide can be confirmed. The unknown sliding surface and topography structure lines can be obtained by interpolation method. Therefore, in the model (Figure 10 *a*), the sliding surface can be regarded as the lower boundary of particles, topography is the upper boundary of particles. By setting a trigger event (strength reduction), these particles

**Table 2.** Factor of safety of Donglingxin landslide

Profile	Sliding mode	Natural	Rainfall	Inundation with rainfall
I-I'	Shallow	1.133	1.085	1.014
	Deep	1.155	1.105	1.023
II-II'	Shallow	1.140	1.077	0.995
	Deep	1.170	1.132	1.035
III-III'	Shallow	1.172	1.127	1.028
	Deep	1.209	1.118	1.045

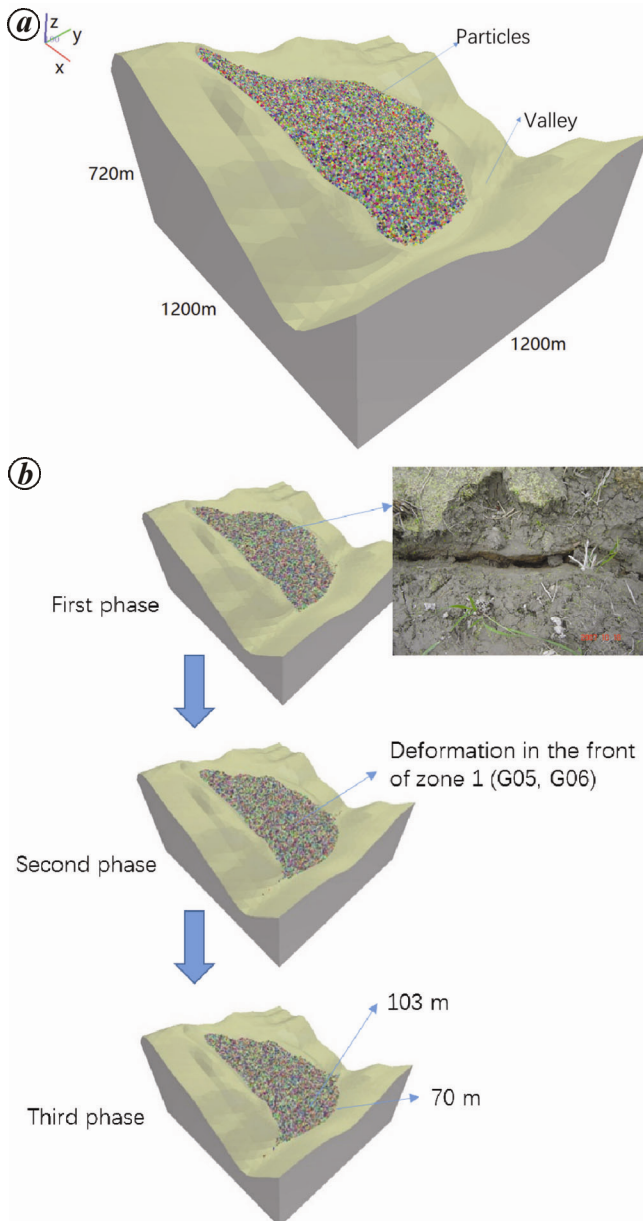


**Figure 10.** The consequence of numerical simulation by YADE. *a*, The computation model; *b*, The evolution of slope deformation.

will drop along the sliding surface due to gravity and accumulate in the valley. Considering the scale of slope, a

calculation model based on topography was built. It was 1200 m both in  $x$  direction (perpendicular to the direction of river) and  $y$  direction (along the direction of river), and 720 m in  $z$  direction (height). There were 45,672 particles in the model, and their diameter ranged from 3 to 6 m. The micromechanical parameters were obtained by simulations of uniaxial compressive test with the targeted elastic properties and saturated strength parameters are listed in Table 1. The suitable micromechanical parameters of particles are presented in Table 3.

The consequence of numerical simulation by using YADE software is shown in Figure 10 *b*. The evolution of slope deformation can be divided into three phases. In the first phase, particles start to slip from the back side of zone 1 where several tension and shear fractures have been observed by *in situ* investigation. In the second phase, particles in the front side of zone 1 collapse and slip to the valley. The deformation in the front side of zone 1 is the largest, as verified by the monitoring data (G05, G06); the particles in zone 2 slip because of the decrease of supporting force. In the third phase, all particles slide down from the slope and not only accumulate in the valley with a maximum height of 103 m, but also on the other side of the valley with a maximum height of 70 m (elevation 490 m). The gradient of accumulation of particles is  $21^\circ$ . The lowest altitude of accumulation (elevation 490 m) is 15 m higher than the reservoir water level (elevation 475 m).

Hence, when Donglingxin slope fails, the Qingshui river will be blocked by stones and soil with the entire debris accumulated in the valley. The water level of upper reaches of the Sanbanxi reservoir will reach 490 m (the elevation of accumulation). The constructions in the upper basin will be in danger. Especially, the Liuchuan town with 22,434 inhabitants which is just about 1.5 km upstream of the slope will be destroyed by surge. The Ji-anhe county town which is 20 km upstream of the slope, with 44,057 inhabitants and 476.6 m in elevation will be destroyed by flood.

The result of simulation is in accordance with the observed deformation and monitoring data, which show that the obvious cracks and fractures appear on the back side of zone 1, especially, in the head of gully. Thus the result obtained from analysis can be used to assess the landslide damage.

**Table 3.** Micromechanical parameters of particles

Density (kg/m <sup>3</sup> )	Elastic modulus (MPa)	Poisson's ratio	<i>c</i> (kPa) (normal direction)	<i>c</i> (kPa) (tangential direction)	$\phi$ (°)
2000.0	100.0	0.35	28–30	28–30	25.5–26.5

This communication presents a case study on deformation characteristics, deformation mechanism of a slope. Emphasis was on the reactivation of Donglingxin landslide induced by precipitation and reservoir fluctuations, as well as a simulation of accumulation patterns of the landslide failure. To sum up, we present the following conclusions:

(i) The Donglingxin slope is a large-scale ancient landslide, formed by several slides along the bank slope, whose vestiges can be found in the toe of the slope. The observed cracks and fractures suggest that the slide is reactivated by reservoir fluctuation, and is a thrust load caused landslide.

(ii) Rainfall and inundation affect different areas of the slope. In the lower part of the slope with high permeability, water infiltrates slope easily and reduces the strength of geological material, so there is obvious deformation in the lower part of slope after inundation. In the upper part of the slope with poor permeability, rain accumulation forms groundwater in the upper part and reduces the strength of geological material. Deformation of the upper part is accelerated after rainfall.

(iii) Stability assessment indicates that the slope would be in critical state. Rainfall and inundation affect different parts of the slope. The shallow sliding surface is influenced by rainfall, while the deep sliding surfaces more is influenced by inundation than rainfall.

The numerical simulation result suggests that the slip appears first in the back side of zone 1 which is in accordance with observed deformation. Then there is a localized landslip in the front side of zone 1 and zone 2 because of the decrease of supporting force. Ultimately the whole slope slips to the valley. Once Donglingxin slope fails, the Qingshui river will be blocked by stones and soil with the total debris accumulated in the valley. The water level of the upper reaches of Sanbanxi reservoir will reach 490 m and hence the constructions in the upper basin will be in danger.

a case study of Wudu County, China. *Arab. J. Geosci.*, 2014, **7**, 1277–1285.

5. Qi, S. W., Yan, F. Z., Wang, S. J. and Xu, R. C., Characteristics, mechanism and development tendency of deformation of Maoping landslide after commission of Geheyan reservoir on the Qingjiang River, Hubei Province, China. *Eng. Geol.*, 2006, **86**, 37–57.
6. Wang, F. W., Zhang, Y. M., Huo, Z. T., Peng, X. M., Araiba, K. and Wang, G. H., Movement of the Shuping landslide in the first four years after the initial impoundment of the Three Gorges Dam Reservoir, China. *Landslides*, 2008, **6**, 321–329.
7. Wang, R. B., Xu, W. Y. and Zhang, J. C., Comprehensive assessment and sliding mechanism analysis of Zhenggang Landslide, Southwestern China. *Disaster Adv.*, 2012, **5**(4), 327–331.
8. Burda, J., Hartvich, F., Valenta, J., Smítka, V. and Rybá, J., Climate-induced landslide reactivation at the edge of the Most Basin (Czech Republic) – progress towards better landslide prediction. *Nat. Haz. Earth Syst. Sci.*, 2013, **13**(2), 361–374.
9. Fleming, R. W., Ellen, S. D. and Albus, M. A., Transformation of dilative and contractive landslide debris into debris flows – an example from Marin County, California. *Eng. Geol.*, 1989, **27**, 201–223.
10. Iverson, R. M., Reid, M. E. and Lahusen, R., Debris-flow mobilization from landslides. *Ann. Rev. Earth Planet. Sci.*, 1997, **25**, 85–138.
11. Baker, R., Determination of the critical slip surface in slope stability computations. *Int. J. Num. Anal. Meth. Geomech.*, 1980, **4**, 333–359.
12. Kozicki, J. and Donzé, F. V., Yade-open dem: an open-source software using a discrete element method to simulate granular material. *Eng. Computation*, 2008, **26**(7), 786–805.
13. Hazzard, James, F. and Young, R. P., Moment tensors and micro-mechanical models. *Tectonophysics*, 2001, **356**(1), 181–197.

ACKNOWLEDGEMENT. This work is financially supported by Fundamental Research Funds for the Central Universities (Grant no. 2014B04914).

Received 13 June 2016; revised accepted 6 February 2017

doi: 10.18520/cs/v113/i06/1159-1166

1. Huang, R. Q., Some catastrophic landslides since the twentieth century in the southwest of China. *Landslides*, 2009, **6**, 69–81.
2. Jin, D. L. and Wang, G. F., Tangyanguang landslide in Zhaxi Reservoir, Hunan Province, China. In *Typical Landslides Occurred in China*, Science Oress, Beijing, 1988, pp. 301–307 (in Chinese).
3. Wang, F. W., Zhang, Y. M., Huo, Z. T., Matsumoto, M. and Huang, B. L., The 14 July 2003, Qianjiangping landslide, Three Gorges Reservoir, China, *Landslides*, 2004, **1**, 157–162.
4. Bai, S. B., Wang, J., Thiebes, B., Cheng, C. and Yang, Y. P., Analysis of the relationship of landslide occurrence with rainfall: